AD-A159 870 POLAR MOMENTS AND BALLISTIC PROPERTIES OF TRI-FOIL PENETRATORS(U) ARMY BALLISTIC RESEARCH LAB ABERDEEN PROVING GROUND MD D N HANSEN SEP 85 BRL-TR-2677 1/1

UNCLASSIFIED F/G 19/4 NL

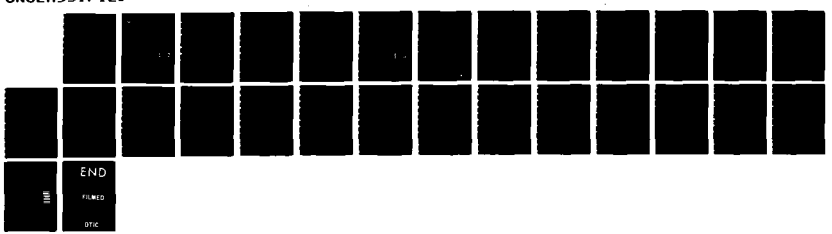

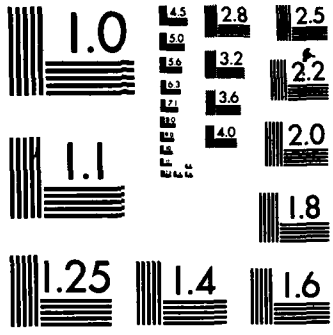

MICROCOPY RESOLUTION TEST CHART
NATIONAL BUREAU OF STANDARDS-1963-A

(12)

AD

AD-A159 870

US ARMY
MATERIEL
COMMAND

TECHNICAL REPORT BRL-TR-2677

POLAR MOMENTS AND BALLISTIC PROPERTIES OF TRI-FOIL PENTRATORS

David N. Hansen

September 1985

US ARMY BALLISTIC RESEARCH LABORATORY
ABERDEEN PROVING GROUND, MARYLAND

Destroy this report when it is no longer needed.
Do not return it to the originator.

Additional copies of this report may be obtained from the National Technical Information Service, U. S. Department of Commerce, Springfield, Virginia 22161.

The findings in this report are not to be construed as an official Department of the Army position, unless so designated by other authorized documents.

The use of trade names or manufacturers' names in this report does not constitute indorsement of any commercial product.

UNCLASSIFIED

SECURITY CLASSIFICATION OF THIS PAGE (When Data Entered)

REPORT DOCUMENTATION PAGE		READ INSTRUCTIONS BEFORE COMPLETING FORM
1. REPORT NUMBER Technical Report BRL-TR-2677	2. GOVT ACCESSION NO AD-A159870	RECIPIENT'S CATALOG NUMBER
4. TITLE (and Subtitle) Polar Moments and Ballistic Properties of Tri-Foil Penetrators		TYPE OF REPORT & PERIOD COVERED Final 6. PERFORMING ORG. REPORT NUMBER
7. AUTHOR(s) David N. Hansen		8. CONTRACT OR GRANT NUMBER(s)
9. PERFORMING ORGANIZATION NAME AND ADDRESS U.S. Army Ballistic Research Laboratory ATTN: AMXBR-TBD Aberdeen Proving Ground, MD 21005-5066		10. PROGRAM ELEMENT, PROJECT, TASK AREA & WORK UNIT NUMBERS 1L162618AH80
11. CONTROLLING OFFICE NAME AND ADDRESS U.S. Army Ballistic Research Laboratory Attn: AMXBR-OD-ST Aberdeen Proving Ground, MD 21005-5066		12. REPORT DATE September 1985 13. NUMBER OF PAGES 26
14. MONITORING AGENCY NAME & ADDRESS(if different from Controlling Office)		15. SECURITY CLASS. (of this report) Unclassified 15a. DECLASSIFICATION/DOWNGRADING SCHEDULE

16. DISTRIBUTION STATEMENT (of this Report)

Approved for public release: distribution unlimited.

17. DISTRIBUTION STATEMENT (of the abstract entered in Block 20, if different from Report)

18. SUPPLEMENTARY NOTES

19. KEY WORDS (Continue on reverse side if necessary and identify by block number)

Penetrators; finned rods; tubular projectiles; multiplate targets; moments of inertia.

20. ABSTRACT (Continue on reverse side if necessary and identify by block number)

Early design tools for tri-foils involved the use of ersatz structures for analysis purposes. This paper presents a method that employs the actual shape to calculate the polar moments of inertia relative to a rod of equal cross sectional area. The method also degrades at its extrema into two logical shapes for this calculation, namely the circle and the equilateral triangle. A ballistic test was performed on a tri-foil having an effective aspect ratio of 14. Performance comparisons with a rod of aspect ratio 16 shows the ballistic performance of the tri-foil to be of the same order but

DD FORM 1 JAN 73 1473 EDITION OF 1 NOV 65 IS OBSOLETE

OVER

UNCLASSIFIED

SECURITY CLASSIFICATION OF THIS PAGE (When Data Entered)

marginally poorer. Systems considerations using tri-foils could make the tri-foil more attractive than the rod. Keywords:

TABLE OF CONTENTS

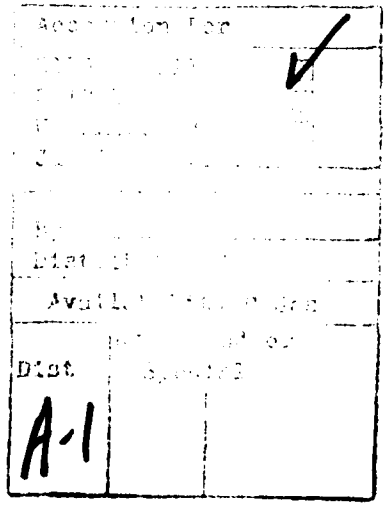

(The following page is blank.)

LIST OF ILLUSTRATIONS

(The following page is blank.)

I. INTRODUCTION

In the middle 1970's the evolution of the long rod munition was accelerating rapidly. Many theoreticians were making predictions of performance and of implementation problems. One of the theoreticians[1] predicted the need for rods of higher stiffness and suggested the implementation of finned rods. He suggested that the shape given in Figure 1 would be of constant polar moment and presented graphs for design purposes. The graphs were not based upon the presented shape; rather they were based upon three planer fins of constant thickness connected at 120°.

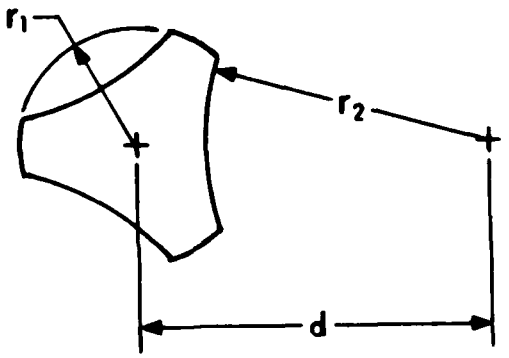

Figure 1. The Katz tri-foil parameters.

We attempted to design two variations of the proposed finned rods and found that we could not duplicate the process by which the original graphs were prepared. Relying solely upon the graphs, two penetrator types were designed with the parameters described in Table 1. These designs were not optimal, and attempts to make optimization computations were frustrated by the lack of a more accurate model.

Table 1. Design Parameters

Item	r_1	r_2	d	L	L/D*
1	8.08	12.12	14.25	96.5	14.6
2	5.41	5.34	7.21	104.8	16.1

Note: Dimensions are in millimeters. The nose was made hemispherical. The length of item 1 was changed to make the weights of each item equal 65 gms. The dimensions given are for the actual rounds since the machinists had difficulty obtaining the design goals.

Our designs were intended for ballistic performance as well as for launch integrity of the rod. The rods were of relatively low L/D*, where D* is the diameter of a circle of the same area as the area of a transverse section of the design. The small aspect ratio of our designs did not require the tri-foil shape for launch or penetration integrity but did allow the study of the foil design with respect to rods that were under study at that time. Each rod was to have an L/D* of 16 but some variations occurred due to machining difficulties. Note that the machinists had fair success with Item 2 but not with Item 1 which had to be shortened to maintain the weight at 65 grams.

Euler[2] buckling of the rod during launch was of greater concern than during the penetration phase. Whereas no closed form solution of the interactions of such a penetrator would be possible for the penetration process, the launch buckling propensity for a tri-foil should be proportional to the relative polar moments of inertia of the rod and foil. For ease of analysis, this ratio will be presented using the model presented in the next section rather than the complete solution of all possible buckling modes. This paper will also present the polar moment for a tubular design for comparison purposes. Other studies involving the tubular design[3 4] have presented the advantages and drawbacks of such projectiles.

II. THE TRI-FOIL SHAPE

The parameters of importance to the tri-foil shape were given in Figure 1. The cutting radii are normalized by the separation distance such that unitless dimensions may be used to describe the designs. It can also be noted that the designs are not limited by the ratio of the fin thickness to the radius (r_1, the fin width) as was the analysis by Katz.[1] If the separation distance between the radii centers becomes very large compared to r_1 the tri-foil will begin to look and behave as a bar with an equilateral triangle for cross section. As less and less is cut from the bar, i.e. r_2 decreases while the other parameters are held constant, the finned bar quickly becomes a rod. The original analysis approached neither of these two limiting cases while the analysis presented in this paper reaches these two realistic limits.

Figure 2 presents the various kinds of geometries that are possible with a simple set of design parameters. The variables k and j are defined after equations 1 and 2 on the following page. A third limiting case with the shape being a hollow cylinder, i.e. d=0, should also be considered. For ease of calculation of the finned shape, the two angles (compare figure 2 and figure 3) were limited to pi/3 radians. This precluded the model from extrapolating to the hollow cylinder and the shapes typified in Figure 2 where k=1.3 and j=0.3. Rather, the closed form solution for the hollow cylinder will be compared as a unique point.

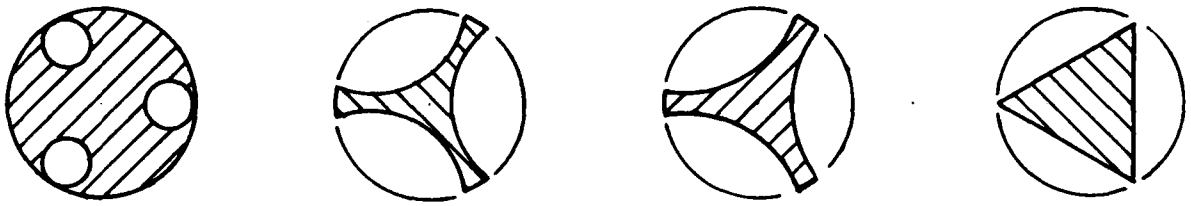

	A	B	C	D
k:	1.3	0.8	0.6	$\ll 1$
j:	0.3	0.8	0.8	≈ 1

Figure 2. Geometries for various values of k and j.

Figure 3 presents the shape used for this analysis. Note that only a third of the total shape is used to simplify the calculation. The simplification comes from the fact that the total polar moment is taken to be just three times the polar moment calculated for this segment. The sector used for normalization is also a third of a circle.

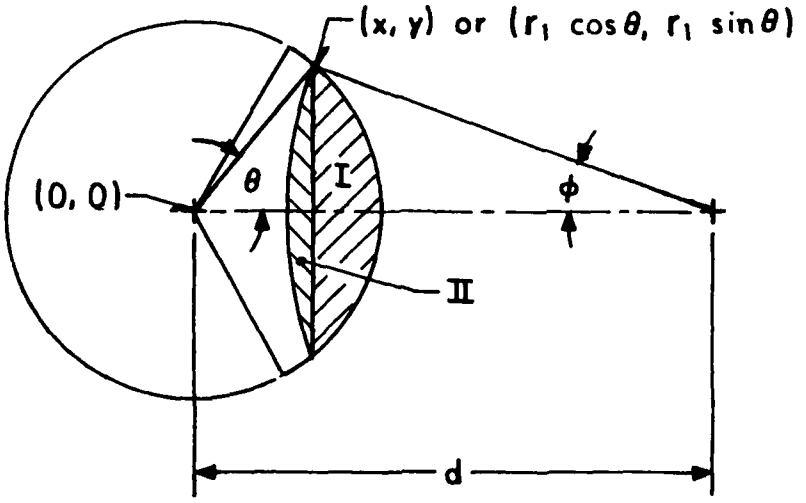

Figure 3. Shape used for the analysis of J/J_o.

Using the following definition of terms:

Theta = Arctan(y/x)
Phi = Arctan[y/(d-x)]

where x and y are derived from the equations for the arcs, namely:

$$x^2 + y^2 = r_1^2 \qquad (1)$$

$$(d-x)^2 + y^2 = r_2^2 \qquad (2)$$

to obtain nondimensionalized parameters the above parameters are divided by d as defined below:

$r_1/d = k$ $r_2/d = j$ $x/d = m$ $y/d = n$

and the equations yield:

$$m = (1 + k^2 - j^2)/2 \qquad m \geq 0 \qquad (3)$$

$$n = \sqrt{(k^2 - m^2)} \qquad (4)$$

Therefore:

Theta = Arctan(n/m)

Phi = Arctan[n/(1-m)] theta and phi: $\leq$ or = $P_1/3$

Solution of the simultaneous equations involving k and the radius, r_1, at theta set equal to Pi/3 and yielding values for n which are less than k times Sin(Pi/3) but greater than zero imply that the foil web would be cut and the foil extrema would be detached; thus, they are rejected in the computer program used to calculate the polar moment ratios. A typical program that will run on a small personal computer is given in the appendix.

Area of sectors and segments as defined in figure 3.

$$Area_T/d^2 = Pi*k^2/3 \qquad (5)$$

$$Area_I/d^2 = k^2*[Theta - Sin(Theta)*Cos(Theta)] \qquad (6)$$

$$Area_{II}/d^2 = j^2*[Phi - Sin(Phi)*Cos(Phi)] \qquad (7)$$

$$Area_N/d^2 = (Area_T - Area_I - Area_{II})/d^2 \qquad (8)$$

for a sector of equal area:

$$Area_O = (Pi * r_o^2)/3 \qquad (9)$$

By definition, the moments of inertia of the tri-foil are to be compared to the moment of inertia of a rod of equal area.

Set: $Area_O = Area_N$

from this the definition of r_o^4/d^4 can be obtained

Polar moments of inertia of the areas defined by figure 3:

$$J_O/d^4 = Pi*r_o^4/(6*d^4) = 3*Area_N^2/(2*Pi*d^4) \qquad (10)$$

The above moment is for the sector of a rod. For the tri-foil a step wise procedure will be followed:

$$J_T/d^4 = Pi*k^4/6 \qquad (11)$$

$$J_I = M_{Ix} + M_{Iy} \qquad J_{II} = M_{IIx} + M_{IIy} \qquad (12)$$

where:

$$M_{Ix}/d^4 = [Theta - Sin(Theta)*Cos(Theta) - 2*Sin(Theta)^3 *Cos(Theta)/3]*k^4/4 \qquad (13)$$

$$M_{Iy}/d^4 = [Theta - Sin(Theta)*Cos(Theta) + 2*Sin(Theta)^3 *Cos(Theta)]*k^4/4 \qquad (14)$$

J_{II} is similar but the y axis must be transferred from the remote position at x = d.

$$M_{IIx}/d^4 = [Phi - Sin(Phi)*Cos(Phi) - 2*Sin(Phi)^3 *Cos(Phi)/3]*k^4/4 \qquad (15)$$

USER EVALUATION SHEET/CHANGE OF ADDRESS

This Laboratory undertakes a continuing effort to improve the quality of the reports it publishes. Your comments/answers to the items/questions below will aid us in our efforts.

1. BRL Report Number _____ Date of Report _____

2. Date Report Received _____

3. Does this report satisfy a need? (Comment on purpose, related project, or other area of interest for which the report will be used.) _____

_____

_____

4. How specifically, is the report being used? (Information source, design data, procedure, source of ideas, etc.) _____

_____

_____

5. Has the information in this report led to any quantitative savings as far as man-hours or dollars saved, operating costs avoided or efficiencies achieved, etc? If so, please elaborate. _____

_____

_____

6. General Comments. What do you think should be changed to improve future reports? (Indicate changes to organization, technical content, format, etc.)

_____

_____

_____

CURRENT ADDRESS

_____
Name

_____
Organization

_____
Address

_____
City, State, Zip

7. If indicating a Change of Address or Address Correction, please provide the New or Correct Address in Block 6 above and the Old or Incorrect address below.

OLD ADDRESS

_____
Name

_____
Organization

_____
Address

_____
City, State, Zip

(Remove this sheet along the perforation, fold as indicated, staple or tape closed, and mail.)

DISTRIBUTION LIST

No. of Copies	Organization
1	Commander US Army Development & Employment Agency ATTN: MODE-TED-SAB Fort Lewis, WA 98433
1	AFWL/SUL Kirtland AFB, NM 87117
1	Air Force Armament Laboratory ATTN: AFATL/DLODL Eglin AFB, FL 32542-5000
1	AFELM, The Rand Corporation ATTN: Library-D 1700 Main Street Santa Monica, CA 90406
	Aberdeen Proving Ground
	Dir, USAMSAA ATTN: AMXSY-D AMXSY-MP, H. Cohen
	Cdr, USATECOM ATTN: AMSTE-TO-F
	Cdr, CRDC, AMCCOM ATTN: SMCCR-RSP-A SMCCR-MU SMCCR-SPS-IL

DISTRIBUTION LIST

No. of Copies	Organization
12	Administrator Defense Technical Info Center ATTN: DTIC-DDA Cameron Station Alexandria, VA 22304-6145
1	HQDA DAMA-ART-M Washington, DC 20310
1	Commander US Army Materiel Command ATTN: AMCDRA-ST 5001 Eisenhower Avenue Alexandria, VA 22333-0001
1	Commander Armament R&D Center US Army AMCCOM ATTN: SMCAR-TSS Dover, NJ 07801
1	Commander Armament R&D Center US Army AMCCOM ATTN: SMCAR-TDC Dover, NJ 07801
1	Director Benet Weapons Laboratory Armament R&D Center US Army AMCCOM ATTN: SMCAR-LCB-TL Watervliet, NY 12189
1	Commander US Army Armament, Munitions and Chemical Command ATTN: SMCAR-ESP-L Rock Island, IL 61299
1	Commander US Army Aviation Research and Development Command ATTN: AMSAV-E 4300 Goodfellow Blvd St. Louis, MO 63120
1	Director US Army Air Mobility Research and Development Laboratory Ames Research Center Moffett Field, CA 94035
1	Commander US Army Communications - Electronics Command ATTN: AMSEL-ED Fort Monmouth, NJ 07703
1	Commander ERADCOM Technical Library ATTN: DELSD-L (Reports Section) Fort Monmouth, NJ 07703-5301
1	Commander US Army Missile Command ATTN: AMSMI-R Redstone Arsenal, AL 35898
1	Commander US Army Missile Command ATTN: AMSMI-YDL Redstone Arsenal, AL 35898
1	Commander US Army Tank Automotive Command ATTN: AMSTA-TSL Warren, MI 48090
1	Director US Army TRADOC Systems Analysis Activity ATTN: ATAA-SL White Sands Missile Range, NM 88002
1	Commandant US Army Infantry School ATTN: ATSH-CD-CSO-OR Fort Benning, GA 31905

List of Symbols (Cont.)

Symbol	Description
$Area_T$	one third of the total area of a rod of radius r_1.
$Area_I$	area of segment defined in figure 3.
$Area_{II}$	area of segment defined in figure 3.
$Area_N$	net area of a tri-foil sector.
$Area_\sigma$	area of a sector of area equal to $Area_N$.
J_σ	polar moment of inertia of a sector of $area_\sigma$.
J_T	polar moment of inertia of a sector of radius r_1.
J_I	polar moment of segment I.
J_{II}	polar moment of segment II.
M	moment about a given axis.
A_N	$Area_N$.
J_c	polar moment of a hollow cylinder.
v_r	residual velocity of largest fragment of penetrator after defeating the target.
v_s	striking velocity of the penetrator.
v_1	probabilistic limit velocity .
A, P	Lambert fit coefficients.

List of Symbols

Symbol	Description
r_1	locii of points that include the extrema of the flanges on a tri-foil or the inner radius of a hollow cylinder depending upon the situation.
r_2	cutting arc which forms the concave curves on the tri-foil surface or the outer radius of a hollow cylinder depending upon the situation.
d	the separation of centers of the tri-foil and the cutting arc.
L	length of a rod or tri-foil.
D	diameter of a rod.
D*	the effective diameter of a tri-foil. i.e. the diameter of a rod with the same area as the tri-foil.
k	the ratio of r_1/d (for a tri-foil).
J	the ratio of r_2/d (for a tri-foil).
Theta	the angle formed between the radius r_1 and the horizontal when r_1 is drawn to end of the chord forming the "missing" segments of the tri-foil. (see figure 3 of text)
Phi	the angle formed between the cutting arc and the horizontal when the cutting arc is drawn to the end of the chord forming the "missing" segments of the tri-foil. (see figure 3)
x	r_1Cos(theta).
y	r_1Sin(theta).
m	x/d.
n	y/d. Note that m and n are used in computer validity checking.

```
 10 PI=3.141593
 20 INPUT "ENTER THE VALUE OF K";K
 30 FOR L=1 TO 100
 40 L2=L/100
 50 M=(1+K^2-L2^2)/2
 60 IF M<0 THEN PRINT "OUT OF RANGE" : GOTO 20
 70 IF M > 1 THEN 400
 80 B=K^2-M^2
 90 IF B<=0 GOTO 400
100 N=SQR(B)
110 T=ATN(N/M)
120 P=ATN(N/(1-M))
130 IF T>PI/3 OR P>PI/3 GOTO 400
140 TN=1+TAN(PI/3)*TAN(PI/3)
150 C=1-(TN*(1-L*L))
160 IF C<0 THEN GOTO 260
170 C1=(1+SQR(C))/TN
180 D=C1*TAN(PI/3)
190 IF D>=K*SIN(PI/3) THEN GOTO 210
200 GOTO 400
210 C2=(1-SQR(C))/TN
220 IF C2<0 THEN GOTO 270
230 D=C2*TAN(PI/3)
240 IF D>=K*SIN(PI/3) THEN 270
250 GOTO 400
260 REM NET AREA IS NORMALIZED BY THE SQUARE OF THE SEPERATION DISTANCE
270 AN=(K*K*PI/3)-((T-SIN(T)*COS(T))*K*K)-((P-SIN(P)*COS(P))*L2*L2)
280 JT=K^4*PI/6
290 REM POLAR MOMENTS ARE ALSO NORMALIZED BY THE SEPERATION DISTANCE
300 J1=K^4/2*(T-SIN(T)*COS(T)+2/3*SIN(T)^3*COS(T))
310 M2X=L2^4/4*(P-SIN(P)*COS(P)-2/3*SIN(P)^3*COS(P))
320 M2YC=L2^4/4*(P-SIN(P)*COS(P)+2*SIN(P)^3*COS(P)-16/9*SIN(P)^6/(P-SIN(P)*COS(P)))
330 M2Y=M2YC+L2^2*(P-SIN(P)*COS(P)-2/3*SIN(P)^3*L2)^2/(P-SIN(P)*COS(P))
340 J2=M2X+M2Y
350 J=JT-J1-J2
360 IF J<0 GOTO 400
370 JN=2*PI*J/3/(AN^2)
380 REM PLOT L2 AS X AND JN AS Y ON A PLOT SCALED FROM 0 TO 1 IN X
390 REM AND 0 TO 7 IN Y.
400 NEXT L
410 GOTO 20
420 END
```

APPENDIX

SAMPLE PROGRAM TO CALCULATE THE RELATIVE POLAR MOMENT RATIOS FOR TRI-FOIL SHAPES

(The following page is blank.)

REFERENCES

1. Katz, J., Long Rod Penetrators, JASON Reports, Technical Note JSR 75-8, November 1975

2. Timoshenko, S. and Gere, J., Theory of Elastic Stability (McGraw-Hill Book Co., New York, NY, 1961)

3. Frank, K. and McLaughlin, R., On the Overall Ballistic Performance of Tubular and Non-Tubular Kinetic Energy Projectiles, U.S. ARMY Ballistic Research Laboratory Technical Report, BRL-TR-02100, September 1978

4. Spinning Tubular Projectile Technology Plan (Preliminary Copy). Prepared by the AD Hoc Spinning Tubular Projectile Committee of the JCTG/MD/WPFG

5. Lambert, J. and Jonas, G., Towards Standardization in Terminal Ballistic Testing: Velocity Representation, U.S. ARMY Ballistic Research Laboratory Report, BRL-R-1852, January 1976

6. Lambert, J., A Residual Velocity Predictive Model for Long Rod Penetrators, U.S. ARMY Ballistic Research Laboratory Memorandum Report, ARBRL-MR-02828, April 1978

7. Private communication with E. Bloore then of BRL.

IV. CONCLUSIONS

The polar moment ratio of tri-foil shaped projectiles has been investigated theoretically. The degree in improvement is marginal but may present some special advantages to the employment of the projectile such as lighter weight sabots or integral fins that may be stripped away by multiple plate targets.

While the ballistic tests were not definitive regarding the use of tri-foil penetrators, they serve to indicate the possible improvements with non circular penetrators. The material was not necessarily up to current standards but by comparing the performance to a rod which was up to the same standard as the tri-foil, relative figure of merit is possible. The ballistic tests were not carried out with the largest possible increases in the polar moment ratio. This was done for two reasons. First, the graphs presented by Katz[1] were not sufficient for accurate design. Second, the lower ratios left much of the mass of the penetrator centralized. Where the mass is left near the center, the impact cross section is maximized. Thus, the performance of the penetrator was not as degraded as would be the case for the shape shown in Figure 5 c, for example.

Some of the designs that are obtainable with unlimited selection of k and j result in shapes that would be extremely difficult to machine, or they would require techniques that are too expensive to permit implementation. These are generally the designs that have flanges at the extrema of the foils. Thus, this investigation centered on "possible" designs by restricting the cutting arc to Pi/3 radians. The same limit had to be applied to the cut arc since a greater angle would result in the outer radius being reduced.

While the ballistic limit of the tri-foil, Item 1, is not as good as the long rod, the performance is very good on a absolute scale. The poorer performance was partly due to the shorter effective L/D of the tri-foil relative to the long rod. Thus, advantages of the tri-foil may be employed without fear of a serious degradation. This presents the fact that should system advantages point to the need of a flanged rod, the tri-foil design can be further developed without large risk factors.

A graphical presentation of the polar moment ratios has been given to permit designing of the tri-foil shape for long rod penetrators. This analysis may also be useful for the design of ornamental columns for structural and architectural purposes. The methods used to calculate this chart, Figure 4, are accurate and the calculation is quick if one has access to a modest computer. Hand calculations are more laborious but readily performed.

velocity, and v_l is the desired limit velocity.

Figure 6 shows the performance of the tri-foil relative to a hemi-nosed rod penetrator of the same material. Note that the A coefficient (see the equation above) of the tri-foil is lower than for the corresponding rod. This results in an asymptote of lower slope and generally infers a better material or design. The higher limit velocity may be highly influenced by the striking velocities and vagaries of this test.

A spectacular behavior was noted during the penetration of the target by the tri-foil penetrator. The extrema of the foils were stripped away by the first and second plates. Item 1 has foils that are narrower at the tip than at any other point. This means that the mass is centered and tends to act like a high aspect ratio rod.

The design of item 2 is such that the fins are thicker at the extrema than at some points along the webs. This can be seen in Figure 7. Note that both designs are drawn to the same scale in this figure. Program limitations prevented the testing of item 2. Ballistic tests should be carried out to determine if the stubbier foils give some of the advantages of long rod penetrators without the disadvantages of tubular projectiles already mentioned.

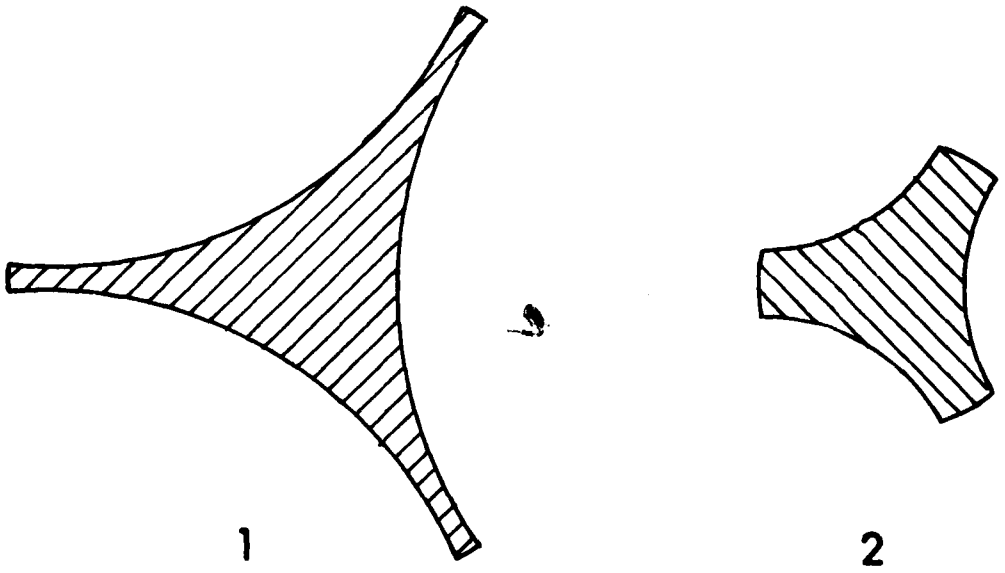

Figure 7. Items 1 and 2 of table 1.

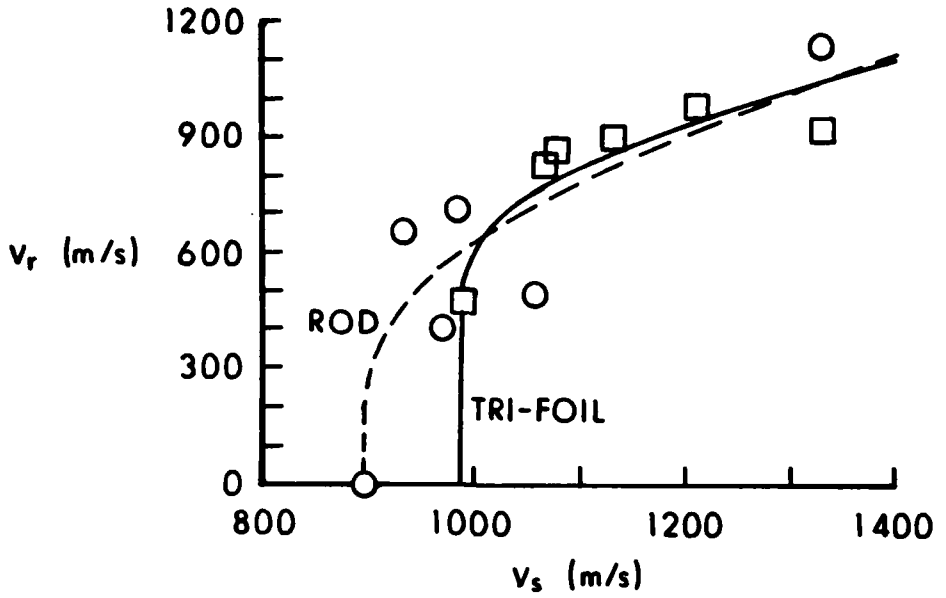

Figure 6. Residual velocity as a function of the striking velocity for the L/D = 16 rod and the L/D* = 14.6 tri-foil. O = rod X = tri-foil

$$v_r = 0 \quad \text{where } v_s < v_1 \qquad (27)$$

v_r is the residual velocity of the largest penetrator fragment passing through the target.
v_s is the initial striking velocity of the penetrator.
v_1 is the probabilistic limit velocity where no penetrations will occur.

and

$$v_r = A(v_s^P - v_1^P)^{1/P} \quad \text{where } v_s > v_1 \qquad (28)$$

A, P, and v_1 thus become the variables that must be fit by multiple regression analysis. A must be positive and less than 1 and P must be greater than 1.

Note that if the variable P is taken as 2, the above equation simply states that the residual energy after penetration is linearly related to the difference between the striking energy and the limiting penetration energy. The implied linearity would be due to a linear decrease in the mass of the residual fragment of the initial rod. By taking P as a variable rather than as 2, the real non-linearity of the process near the limit velocity can be fit. While this does not qualify as a model, the high degree of freedom experienced by having three variables to fit results in very good fits. The variable A is related to the asymptote that the data approach when the target is severly overmatched. P relates to the degree of curvature near the limit

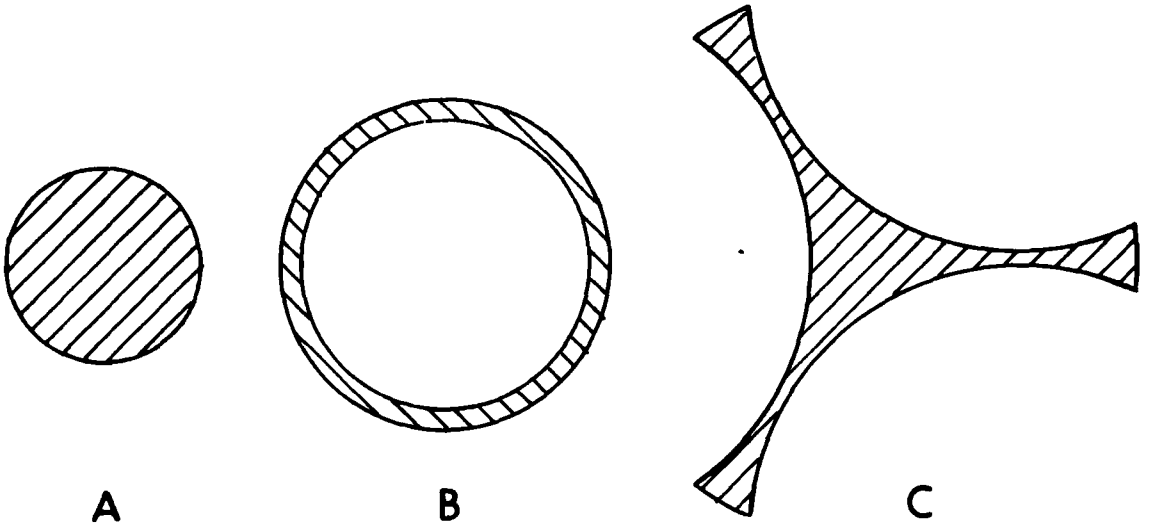

Figure 5. Constant area shapes. B and C have polar moment ratios of 5.1 relative to A.

III. BALLISTIC TEST

A comparison ballistic test was performed using one of the two designs listed in Table 1. The tri-foil was compared to a simple rod penetrator having a hemispherically rounded nose. Both the rod and foil shapes were made from U-3/4 Ti alloy. This is a high ductility, high density material which was heat treated similarly to the M774 penetrator material. The simple rod had an L/D of 16 which was also the target L/D* for the tri-foil shapes. Due to machining difficulties the desired dimensions could not be held, and they were modified by the vendor for Item 1. This modification led to a slightly over weight penetrator. To correct the weight, Item 1 was again modified by cutting off some of the length. The target was a standard US triple target.

The strikes that were considered valid are presented in Figure 6. This plot assumes that the penetration process will result in a penetration curve[5] see equations 27 and 28 below, that has the solution as given by Lambert.[6] Lambert's curve fitting passes through the center of the data rather than following Bloore's hypothesis[7] that all data should be below and to the right of the curve.

The polar moment of inertia for a hollow cylinder is easily obtained from:

$$J_c = Pi*(r_2^4 - r_1^4) \qquad (22)$$

for a hollow cylinder of inner radius r_1 and outer radius r_2

$$J_o = Pi*r_o^4 \qquad (23)$$

for a rod of radius r_o

As above, define the area of the rod to equal the area of the cylinder such that:

$$r_2^2 - r_1^2 = r_o^2 \qquad (24)$$

thus:

$$J_c/J_o = (r_2^2 + r_1^2)/r_o^2 \qquad (25)$$

and we have:

$$r_2/r_o = \sqrt{[(J_c/J_o/2) + 1/2]} \qquad (26)$$

Comparison of a hollow cylinder with the tri-foil can be made for specific polar moment ratios. That is, if we choose a hollow cylinder with a polar moment ratio of 7, for example. The above equations quickly show:

$$r_2/r_o = 2 \text{ and } r_1/r_o = \sqrt{3} \quad \text{for the cylinder}$$

and for the tri-foil k and j must be selected from Figure 4 of the text, k = 0.85 and j about 0.864 should give the desired ratio of moments of inertia. Note, the author has done some calculations to obtain these values of k and j; J/J_o is actually about 6.9 for these parameters; a closer definition of k and j to exactly achieve 7 is unrealistic in terms of machining tolerances.

The usual criterion of equal area defines r_1, r_2, and d for the tri-foil.

$$r_1/r_o = 3.53 \qquad r_2/r_o = 3.60 \qquad \text{and} \qquad d/r_o = 4.16$$

where: r_o is the basic radius of the solid rod.

Another such comparison is presented in Figure 5 relative to a rod of unit radius.

$$M_{IIy'}/d^4 = [Phi - Sin(Phi)*Cos(Phi) + 2*Sin(Phi)^3 *Cos(Phi)]*j^4/4 \qquad (16)$$

$$M_{IIy,c}/d^4 = M_{IIy'}/d^4 - A*x^2/d^4 \qquad (17)$$

where: $$x/d = 2*j*Sin(Phi)^3/[Phi - Sin(Phi)*Cos(Phi)] \qquad (17)$$

and $$A/d^2 = j^2*[Phi - Sin(Phi)*Cos(Phi)] \qquad (18)$$

$$M_{IIy}/d^4 = M_{IIy,c}/d^4 + A*(1 - x/d)^2/d^2 \qquad (19)$$

$$J_N/d^4 = (J_T - J_I - J_{II})/d^4 \qquad (20)$$

and $$J/J_o = 2*Pi*J_N/d^4/[3*(A_N/d^2)^2] \qquad (21)$$

where: A_N is the net area.

A computer program was written to calculate the ratio of polar moments; and the results are shown in Figure 4. The intersection at the left of the graph at 1 is the natural limit where the tri-foil acts as a rod. The locii of the terminus points of the various curves point to the value of the polar moment ratio for a cross section of an equilateral triangle. Since this program was run with a coarse step the terminus points are not exact and extrapolation with respect to the graph is not very accurate. This value can be easily calculated from the equations given above.

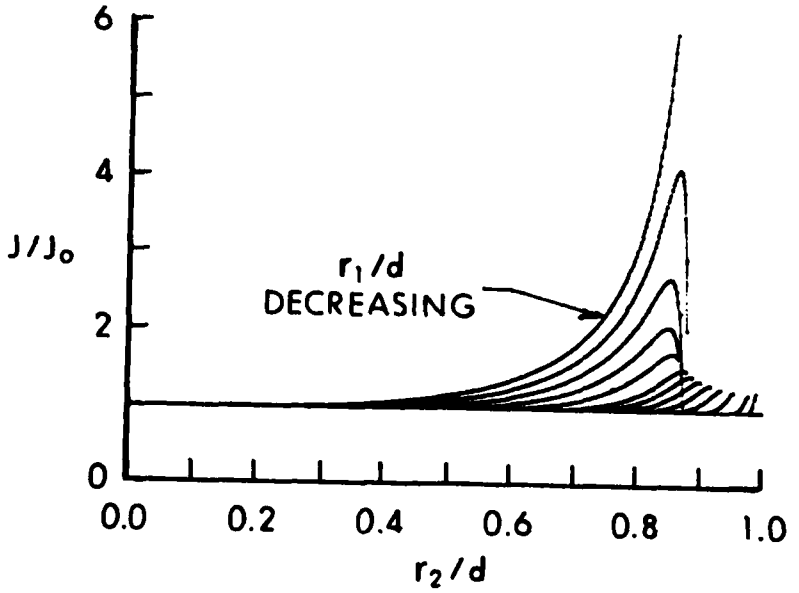

Figure 4. Relative polar moment, J/J_o, as a function of r_2/d. Curves are for r_1/d ratios of .85, .75, .65, .55, .45, .35, .30, .25, .20, .15, .10, .05, and .025 going from left to right.

— — — — — — — — — — FOLD HERE — — — — — — — — — —

Director
US Army Ballistic Research Laboratory
ATTN: AMXBR-OD-ST
Aberdeen Proving Ground, MD 21005-5066

NO POSTAGE
NECESSARY
IF MAILED
IN THE
UNITED STATES

OFFICIAL BUSINESS
PENALTY FOR PRIVATE USE, $300

BUSINESS REPLY MAIL
FIRST CLASS PERMIT NO 12062 WASHINGTON, DC
POSTAGE WILL BE PAID BY DEPARTMENT OF THE ARMY

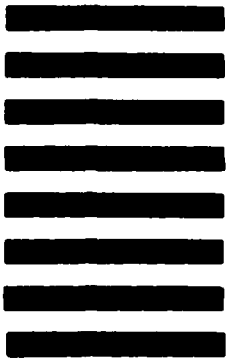

Director
US Army Ballistic Research Laboratory
ATTN: AMXBR-OD-ST
Aberdeen Proving Ground, MD 21005-9989

— — — — — — — — — — FOLD HERE — — — — — — — — — —

END

FILMED

11-85

DTIC